



Restoration of above canopy reference hemispherical image from below canopy measurements for plant area index estimation in forests

Mait Lang^{1,2*}, Ave Kodar³ and Tauri Arumäe¹

Lang, M., Kodar, A., Arumäe, T. 2013. Restoration of above canopy reference hemispherical image from below canopy measurements for plant area index estimation in forests. – Forestry Studies | Metsanduslikud Uurimused 59, 13–27. ISSN 1406-9954. Journal homepage: <http://mi.emu.ee/forestry.studies>

Abstract. Canopy gap fraction has been estimated from hemispherical images using a thresholding method to separate sky and canopy pixels. The optimal objective thresholding rule has been searched by many authors without satisfactory results due to long list of reasons. Some recent studies have shown that unprocessed readings of camera CCD or CMOS sensor (*raw data*) have linear relationship with incident radiation. This allows a pair of cameras used in similar to a pair of plant canopy analyzers and canopy gap fraction can be calculated as the ratio of below canopy image and above canopy image. We tested new freeware program HemiSpherical Project Manager (HSP) for the restoration of the above canopy image from below canopy image which allows making field measurements with single below canopy operated camera. Results of perforated panel image analysis and comparison of plant area index (PAI) estimated independently by three operators from real canopy hemispherical images showed high degree of reliability of the new approach. Determination coefficients of linear regression of the PAI estimations of the three operators were 0.9962, 0.9875 and 0.9825. The canopy gap fraction data obtained from HSP were used to validate Nobis-Hunziker automatic thresholding algorithm. The results indicated that the Nobis-Hunziker algorithm underestimated PAI from out of camera JPEG images and overestimated PAI from *raw data*.

Key words: hemispherical images, canopy, gap fraction, LinearRatio, leaf area index.

Authors' addresses: ¹Tartu Observatory, 61602 Tõravere, Tartumaa, Estonia; ²Institute of Forestry and Rural Engineering, Estonian University of Life Sciences, Kreutzwaldi 5, Tartu 51014, Estonia; ³Faculty of Science and Technology, University of Tartu, Vanemuise 46, Tartu 51014, Estonia; *e-mail: mait.lang@emu.ee

Introduction

Green leaves on plants are remarkable organs that have been influencing the Earth's history and climate via absorption of solar energy and CO₂ for photosynthesis at the same time releasing oxygen, volatile organic components and transpiring water (Beerling, 2012). The amount of ab-

sorbed photosynthetically active radiation by plant canopies is an important quantity that characterizes the intensity of the photosynthesis (Tooming, 1977).

Atkins *et al.* (1937) used photoelectric cells to measure incident radiation in an open field I_o and below forest I_b at the same time and applied the "daylight factor" $T = I_b / I_o$ to describe the amount of energy

reaching forest floor. The daylight factor can be calculated separately for diffuse and direct radiation, due to different impact for photosynthetic and respiration process (Niinemets *et al.*, 2001). In one hand, such instrumental measurements were objective and provided directly physical quantities of the energy; on the other hand, the method required two calibrated sensors, near-by open field and longtime measurements to obtain estimates of T for all possible illumination conditions. Evans & Coombe (1959) tested upward pointed camera with a special lens capable of recording image just over the hemisphere in woodlands. The hemispherical images could later be used to predict sunspots on the forest floor and to analyze the possible dependence of the daylight factor on distribution of gaps in the canopy. Evans & Coombe (1959) pointed out the complex nonlinearity of photochemical processes and light scattering within lens and camera as the main obstacles for the film based photography to replace instrumental measurements described by Atkins *et al.* (1937).

The modern definition of hemispherical photography for light climate studies in plant canopies was established by Anderson (1964), who divided image into small annuli by azimuth and zenith and assigned percentage of obscured sky for each annulus according to visual interpretation. After criticizing the ambiguous use of daylight factor, Anderson (1964) proposed a new term "site factor" as percentage of total (diffuse plus direct) light at a given site compared with total light in the open over the same period. Additional qualifications to distinguish for total, diffuse, direct, instantaneous etc., were proposed for the site factor, however the basic idea was the same as that of daylight factor. Remarkably good agreement between directly instrumentally measured irradiance and site factor based irradiance estimate at the three woodland sites proved the reliability of the hemispherical images based canopy transmittance estimates. The variation of diffuse

sky luminance was described by using a theoretical model (Anderson, 1964).

In plant canopies the extent of photosynthesis is determined by the amount of green leaves containing chlorophyll. Watson (1947) studied crop yield of sugar beets and defined leaf area index (LAI) as the total one sided area of leaf tissue per unit ground surface area. The LAI, simple by its definition, is difficult to measure in most of plant canopies. One of the first reliable LAI estimation methods was inclined point quadrats based on counting contacts of foliage with thin long needles passed through canopy (Wilson, 1960). Nilson (1971) used theoretical models that related foliage geometry to the mean proportion of gaps (gap fraction) P_0 in canopy in the view direction and explained the different values of extinction coefficient in common relationship

$$P_0 = \exp(-kLAI) \quad (1)$$

where k is extinction coefficient. The Eq. (1) connects hemispherical photography to leaf area index estimation if the images are taken in the spectral region where plant elements are opaque and not reflecting i.e. black and sky radiance is high (Kuusk *et al.*, 2002, Jonckheere *et al.*, 2004). Such conditions are fulfilled for blue spectral region and diffuse incident radiation I_D (Welles & Norman, 1991). Here the gap fraction can be expressed in similar to Atkins *et al.* (1937) as $P_0 = T = I_{Db}/I_{Da}$ where I_{Da} and I_{Db} are the above and below canopy measurements, and the relationship is used e.g. in plant canopy analyzer LAI-2000 (Welles & Norman, 1991). To estimate the true green leaf area index as defined by Watson (1947) from gap fraction measurements for forest canopies one needs to apply sophisticated theoretical models to account for foliage clumping and the effect of trunks and branches (Nilson & Kuusk, 2004; Leblanc *et al.*, 2005; Ryu *et al.*, 2010; Pisek *et al.*, 2011). Without applying any corrections one can estimate plant area index PAI directly from canopy transmittance T data

$$PAI = -2 \int_0^{\pi/2} \ln(T(\theta)) \cos \theta \sin \theta d\theta \quad (2)$$

where $T(\theta)$ is azimuthally averaged transmittance at view zenith angle θ .

Development of digital scanning devices and small computer systems introduced new era in hemispherical photography processing (Rich, 1990). Pixels of digital images could now be fast classified according to a threshold into sky and plant classes corresponding to binary values sky = 1 and plant = 0. A canopy average gap fraction can be calculated from thresholded binary images with computer programs using sampling schema in similar to Anderson (1964). However & Rich (1990) pointed out the subjectivity of operator when selecting threshold for image classification. Subjective threshold combined with complex nonlinearity of photographic film, the issue raised already by Evans & Coombe (1959), lead Rich (1990) to express desire for a compact hemispherical imaging device with on-board digitizing and image processing capabilities. No more than ten years later digital compact cameras were freely available on the market and were also used to record hemispherical images. In hand with the digital data availability, several software programs were developed to process hemispherical images and to extract canopy structural information (Jonckheere *et al.*, 2004). Such programs for processing digital hemispherical images as GLA (Frazer *et al.*, 1999), CIMES (Walter, 2009), CAN-EYE (Weiss, 2013), hemispher (Schleppi *et al.*, 2007) or DHP (Leblanc *et al.*, 2005) are freely available for download over the internet. However, the problem of signal non-linearity was still as persistent as it was during the photographic film era (Evans & Coombe, 1959), since the consumer grade digital compact cameras do automatically and nonlinearly change their quantum sensor's signal to adopt the output image for human vision. The camera-specific image processing in digital cameras adds uncertainty related to image

acquisition settings (Inoue *et al.*, 2004) - i.e. the same problems that were never fully solved for film cameras (Anderson, 1964; Macfarlane *et al.*, 2000). Also, Jonckheere *et al.* (2004) again pointed out in their review paper the unsolved issue of subjectivity of threshold based methods for gap fraction estimation. On the other hand, Macfarlane *et al.* (2007a) proposed regular digital images instead of hemispherical images to estimate canopy cover and crown porosity for effective plant area index estimation and Macfarlane *et al.* (2007b) applied the method successfully for eucalyptus stands where destructive sampling based maximum LAI was 2.83. The method proposed by Macfarlane *et al.* (2007a) requires separation of gaps between crowns from the gaps within crowns which was done manually.

Jonckheere *et al.* (2005) carried out comprehensive study on automatic image thresholding methods to replace subjective operator decision. The results, however, did not bring clearly up one particular best algorithm maybe due to the fact that Jonckheere *et al.* (2005) used the regular, human vision adopted digital images. An unresolved issue when thresholding hemispherical images is the view direction dependent variability of incident radiation (Anderson, 1964) since during both favorable diffuse illumination conditions - overcast and clear sky during sunset or sunrise, incident radiation has a strong dependence on view direction and on the Sun position (Kittler, 1994).

The method for proper use of modern digital cameras for hemispherical imaging of forest canopies was published by Cescatti (2007), who suggested the use of camera quantum sensor *raw data* instead of regular images. Cescatti (2007) placed one camera in an open area and measured penetrated radiation below forest canopy with the second camera similar to the measurement setup of Atkins *et al.* (1937), and calculated canopy transmittance $T = I_{Db}/I_{Da}$ and called the method LinearRatio. The agreement of

the image based T with plant canopy analyzer LAI-2000 data based T proved linearity of camera *raw data*. The two sensor setup is not practical for measurements in forest where nearby sufficiently large open areas are not available. Lang *et al.* (2010) showed that by using signal from gaps in canopy the above canopy hemispherical image can be restored from the below canopy image and the LinearRatio method of Cescatti (2007) can be adopted for a single below canopy operated digital camera. The single camera based LinearRatio has clear advantages, since there is no need to synchronize or calibrate two sensors and errors inherent in illumination variability as reported already by Anderson (1964) are avoided.

The aim of the paper is to introduce and test HemiSpherical Project Manager – free software utility that implements canopy gap fraction calculation from digital hemispherical images by using the LinearRatio for single camera. The main processing steps are described starting from image extraction from *raw data* files followed by image correction for vignetting and projection distortions, above canopy image restoration and finally export of the results. The procedures were tested using 1) an image of perforated panel and 2) below canopy images from forest growth sample plots (Hordo *et al.*, 2006) processed by three independent operators. Finally, the results were used to validate sample plot level PAI estimates based on gap fraction estimates from Nobis & Hunziker (2005) automatic thresholding algorithm.

Material and Methods

Description of HemiSpherical Project Manager software

The HemiSpherical Project Manager (HSP) is written in java and therefore is virtually independent from operating system. Image processing is carried out in three basic steps 1) image extraction from camera *raw data*

files, 2) restoration of above canopy hemispherical image and 3) export of results.

The HSP uses free software utility *dcraw* (Coffin, 2013) to extract unprocessed sensor data from camera specific *raw data* files. Unprocessed means no scaling and no interpolation of pixel values over sensor with *Bayer* filter, the procedure used for digital cameras to create colour image from array of individual pixels (sensor) recording only red, green or blue radiance (Lebourgeois *et al.*, 2008; Lang *et al.*, 2010). If needed, then dark current signal (i.e. an image of completely covered optics) can be subtracted during image data import. Some cameras have significant dark current signal while others do not (Lang *et al.*, 2010). After *dcraw* has imported the sensor images from camera specific *raw data* files, further analysis is carried out in HSP to extract the pixels with original blue filter according to the camera filter pattern, to correct for lens and camera vignetting, correct for projection model and resample images into a common dimensions. The last is useful if images from different cameras are to be processed for the same sample plot.

Next step for gap fraction estimation according to the rule $P_0 = I_{Db}/I_{Da}$ is to restore above canopy hemispherical image from the below canopy measurement. Assuming a linear relationship between incident radiation and digital sensor pixel values extracted from *raw data*, the simplest way to restore the above canopy image is to interpolate the sky pixel values taken from the canopy gaps (Lang *et al.*, 2010). For each open sky mark the mean value of 3 by 3 pixel window is calculated from image as a sample. For interpolation in HSP, inverse distance is used as a weight. User can select the number of nearest sky markers to be used for interpolation and maximum search distance of sky markers around pixel. The interpolation method is useful to account for local variability of incident radiation in hemispherical images.

Second option to restore above canopy hemispherical image is by using a mathe-

mathematical model of sky radiation (Lang *et al.*, 2010). Anderson (1964) used mathematical model of overcast sky radiation distribution for the site factor dependent energy transmission calculations. Kittler (1994) proposed a sky radiation distribution model that accounts for Sun position and estimates relative sky radiation for any view direction of hemisphere in respect to view zenith. International Organization for Standardization has published fifteen so called standard models (CIE, 2004) based on work of Kittler (1994). The CIE (2004) model is based on a single equation with five adjustable parameters *a...e*, the values for standard models are given in lookup table. Since the standard cases are hardly found during real measurement situation, HSP has an option to fit the CIE (2004) model parameters *a...e* using the sky samples. Due to the high degree of nonlinearity, the result of the model parameter fitting depends somewhat on initial solution. User can select standard CIE (2004) models as starting points and is recommended to consider the in situ observations of sky conditions made in the field during imaging to find the best model. The mathematical model requires data of Sun position and sky radiance value in zenith direction. Since mathematical model ignores local variability caused by clouds, the optimal solution in practical image processing is to mix interpolation and mathematical model for above canopy hemispherical image restoration (Lang *et al.*, 2010). The algorithm accounts for maximum search distance of sky samples in interpolation and for those pixels outside the search distance only the model estimate is used.

In third step, HSP provides several options to export gap fraction data from individual images or as an average over several images. The list of export formats includes azimuthally averaged gap fraction stored into simple ASCII text file, gap fraction data as portable gray map image or bitmap file (BMP) or CanEye package.

Tests with perforated panel image

The idea to measure an artificial target or a structure to validate optical methods and corresponding equipment for LAI estimation can be found from Welles & Normann (1991) and from Song *et al.* (2014). We used an image of black painted and circular holes perforated panel (Ducksoo Industrial Company Ltd., Seoul, South Korea) which according to manufacturer's estimate had gap fraction value $P_0 = 0.4030$. The image was taken with regular lens on a cloudy day with Canon EOS 600D and Canon EFS 18–55 mm regular lens, aperture fixed to f/8.0, ISO speed set to 100 and shutter speed was set to 1/1024.0 seconds. The camera was not calibrated in radiometric lab, hence the equidistant projection model and no vignetting were assumed. The settings provided the maximum signal of 6975DN after dark frame subtraction which is significantly less than the saturation value of the camera sensor. The panel image file and accompanying dark frame image file was kindly provided by prof. Youngryel Ryu from Department of Landscape Architecture and Rural Systems Engineering, Seoul National University, Seoul, South Korea.

A circular subset was extracted from the panel image in HSP and stored as 1730 × 1730 pixel matrix (Figure 1, a). The image area contained 179 full or partial holes and into each hole one sky marker was placed. In the first test only interpolation using three nearest sky markers to pixel and maximum search distance of 200 pixels was carried out for unobscured sky image restoration (Figure 1, b). In the second test 10 random samples each containing 17 sky markers was drawn and on each sample mathematical sky model was fitted and mixed with interpolation to restore unobscured sky image. The model weight was set to 1%. For the image pixels that did not have clear sky markers within search distance only the model estimate was used. The brightest spot in the image was used for Sun position and zenith radiance value

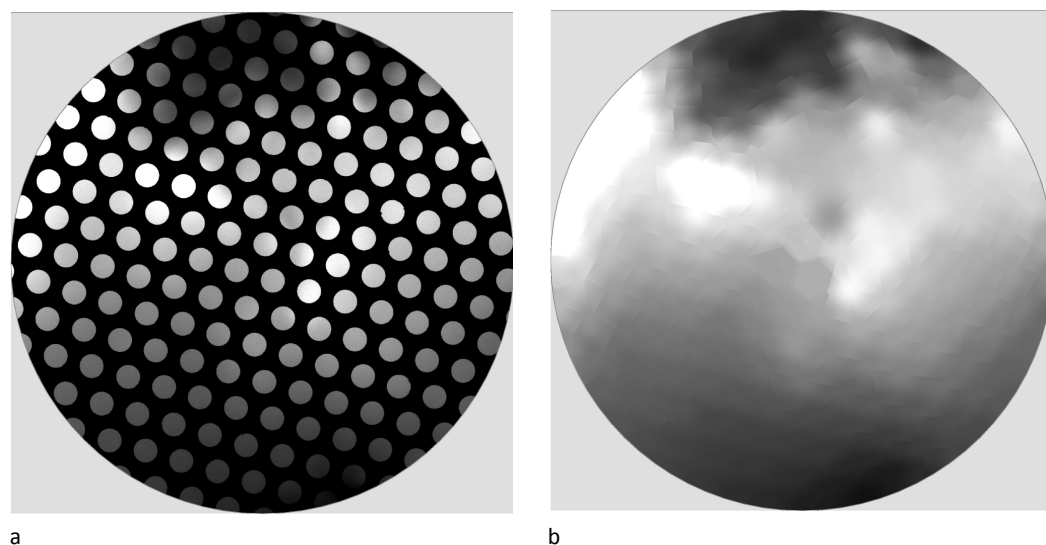


Figure 1. A subsample of perforated panel image taken with cloud covered sky as a background (a) and restored unobscured sky by using interpolation of pixel values from the holes (b).

Joonis 1. Väljalõige pilvise taeva taustal pildistatud aukudega musta värvi paneelist (a) ja aukudest võetud pikslite väärtuste interpoolimise abil taastatud taeva kujutis (b).

was set manually, since random samples do not ensure sky markers in the near zenith area (image centre). The gap fraction estimate was calculated for each sample of points for the panel image in the second test. For comparison, an automatic thresholding algorithm of Nobis & Hunziker (2005) was applied to the panel image outside HSP. The algorithm was first unable to find an optimal threshold, since few extremely bright pixels established small second mode of brightness histogram. This problem was solved by allowing the algorithm to update the optimal value only if the number of detected edges for a virtual image level was more than the number of the image columns.

Hemispherical canopy images

In Laeva, Estonia, six forest growth sample plots were measured from May to June 2013 (Table 1). The forests were growing on *Aegopodium* site type (Lõhmus, 2004). Two digital cameras were used – Nikon D5100 with Sigma's 4.5 mm F2.8 EX DC

HSM Circular Fisheye and Canon EOS 5D with a Sigma 8mm 1:3.5 EX DG Fisheye lens. On each forest growth sample plot 12 fisheye photographs were taken: 3 photos were taken in 4 different cardinal directions (North, South, East and West), with a distance of approximately 4 meters between each take. The schema for measurements was adopted from VALERI project (Validation of Land European Remote sensing Instruments, <http://www.avignon.inra.fr/valeri/>). Usually, we operated two cameras at the same time on a forest growth sample plot, so that both cameras took 6 hemispherical images from 2 different cardinal directions. All images were recorded at approximately breast height level (1.3 m) and cameras were fixed on tripods the way that optical axis's of the lenses were pointed to zenith, and the bottom of both cameras was oriented to South direction. The measurements were done on evenings, when the illumination was diffuse. When there was need to avoid local sensor saturation by directly look-

Table 1. Main characteristics of forest growth sample plots. Roman numbers I, II denote the upper and lower layer of trees. The forests are characterized by basal area (G), stand mean height (H), stand density (N) and age (A). Tree species are coded: HB – *Populus tremula* L., KS – *Betula pendula* R., KU – *Picea abies* L., RE – *Salix caprea* L., LM – *Alnus glutinosa* L.

Tabel 1. Proovitükkide puistute kirjeldus rinnaspindala (G), puistu valitseva rinde keskmise kõrguse (H), puistu tiheduse (N) ja vanuse (A) järgi. Puuliikide lühendite selgitus on ülal. Rooma numbrid liigilise koosseisu valemis tähistavad rindeid.

ID	Species composition / Puistu koosseis	G, m ² ha ⁻¹		H, m		N, t ha ⁻¹		A, y
		I	II	I	II	I	II	
313	I: 53 KS 44 HB 3 KU II: 97 KU 3 KS	28.7	16.3	32.6	19.7	372	672	80
314	I: 75 HB 25 KS II: 88 KU 12 KS	25.0	13.6	32.8	17.5	236	609	80
315	I: 78 HB 18 KS 4 KU II: 100 KU	35.8	13.0	33.6	18.3	314	629	90
316	I: 57 KS 30 HB 13 KU II: 97 KU 3 KS	28.0	11.8	31.8	14.5	382	835	80
317	I: 55 HB 25 KS 20 KU II: 78 KU 22 KS	36.7	13.0	30.2	17.5	552	835	80
318	I: 55 HB 32 KU 11 KS 1 RE 1 LM II: 100 KU	33.2	6.7	28.4	19.1	581	357	67

ing at the low Sun, recording location was shifted (about +/- 1m) to block the Sun by a near-by tree trunk. The image brightness histogram was observed to avoid overexposure of the images. At each sample plot one dark current image was taken. All the image sets were taken on 4–5 different dates to get the phenological changes in the forest canopy (see Figure 2). We recorded images on May 6th, 13th, 20th and 27th and June 10th for IDs 313, 314, 315 and 318; for IDs 316–317 we took pictures only during May.

Tests with hemispherical images processed by three operators

Three independent operators processed the set of Laeva test site sample plot images using the HSP software. The only restriction was the CIE model weight set no bigger than 0.3 when mixing CIE model with interpolated data for above canopy image restoration. Plant area indexes for each sample plots – for each measurement date and for each operator – were calculat-

ed according to Eq. (2). We used the PAI to assess the influence of operator's decision on the above sky restoration method for LinearRatio.

The spatial resolution of hemispherical images decreases with increasing view zenith angle (Leblanc *et al.*, 2005) and the fraction and size of gaps decreases also. This can cause operators to place the sky markers occasionally on small gaps with mixed pixels. As a result the calculated gap fraction will be overestimated around this marker. Such wrong placed sample points have an influence to the fitting of CIE model parameters too. To estimate the influence of possible errors of sky radiance sample points which could have been placed into the gaps with mixed pixels, we reprocessed plot level measurements after removing all such initially placed sample points.

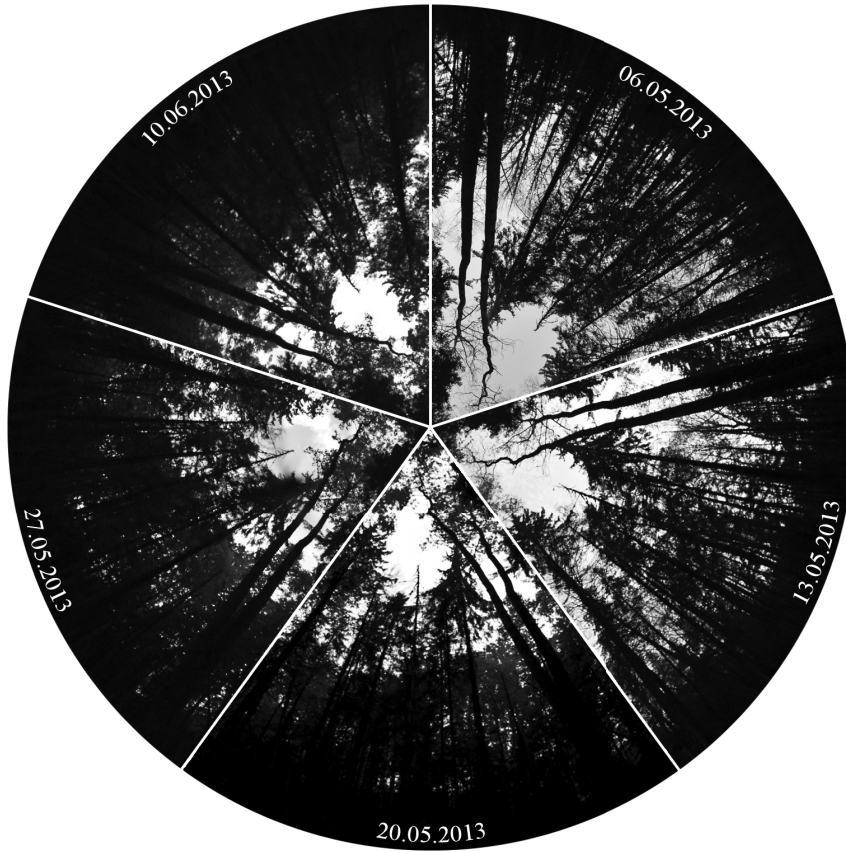


Figure 2. Illustrative overview of the phenological changes occurred in the forest canopy from May, 06th till June, 10th in sample plot 318.

Joonis 2. Võrastikus toimunud fenoloogilised muutused proovitükil 318 ajavahemikus 06. mai kuni 10. juuni.

Validation of the Nobis-Hunziker thresholding algorithm

Nobis & Hunziker (2005) automatic thresholding algorithm with similar constraints as for the panel image was used to classify the blue channel image of camera output JPEG files and images of blue pixels extracted from *raw data*. The JPEG files were initially collected in parallel to raw data for quick look purposes. Compression ratio was set smallest to keep as much color information as possible. Camera defaults were used for the other settings. The radius of hemispherical image was 994 pixels in the Nikon D5100 images and 1436

pixels in the Canon EOS 5D images. Jpeglib library for pascal was used to decompress the JPEG files. The PAI was calculated for each dataset using Eq. (2). Since binarized JPEG-s had sometimes all pixels set to $T = 0$ at large zenith angles, pixels in all images from the zenith angle more than 78.5 degrees were excluded in this test. The automatic thresholding based PAI was validated by using the PAI based on gap fraction data obtained from HSP.

Results and Discussion

The estimated gap fraction of the perforated panel was $P_0 = 0.3792$ if all 179 sky marks were used for interpolation method to restore clear sky image. This is 5.9% smaller compared to the value given in manufacturers documentation ($P_0 = 0.4030$). The difference can be explained by small defects at the edges of the circular holes and the small 5.9% deviation may be fully in agreement with confidence intervals of the panel specification. The sky marker sampling experiment where interpolation and sky radiation model was used gave the mean gap fraction value $P_0 = 0.3826$ and standard deviation $S_{P_0} = 0.0114$. This test proved the above canopy unobscured sky image restoration method's reliability in case of dense forest canopies where only few gaps are present. The test indicated also flexibility of the CIE (2004) model, since originally developed for hemispherical images the model performed well for the panel image subsample. For comparison to manual methods we tested also a fully automatic algorithm of Nobis & Hunziker (2005), which had performed well in LAI estimation from downward looking planar images taken over snow covered ground and boreal forest (Manninen *et al.*, 2009). The Nobis-Hunziker algorithm found an optimal threshold equal to 1315 DN which gave gap fraction estimate $P_0 = 0.3696$ for the panel subsample.

The subjectivity of an operator determining an optimal threshold for hemispherical image for gap fraction estimation has been an unsolved problem (Jonckheere *et al.* 2004). We arranged an operator influence study on the above sky restoration method for LinearRatio by using hemispherical images taken during rapid phenology change (Figure 3) in forest growth sample plots.

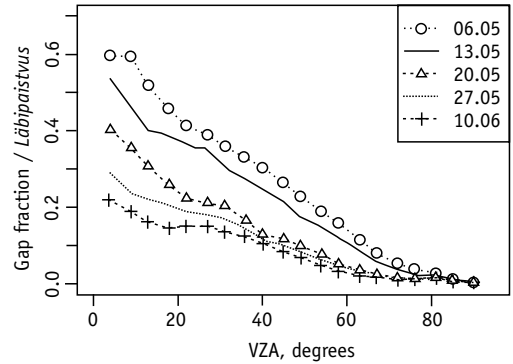


Figure 3. Change of gap fraction angular dependence in sample plot 318 from May, 06th till June, 10th. See also Figure 2.

Joonis 3. Läbipaistvuse muutus proovitükil 318 ajavahemikus 06. mai kuni 10. juuni. Vaata ka joonist 2.

The estimates of plant area index based on three different operators agreed well and were not biased in respect to each other (Figure 4). The high R^2 values (0.9962, 0.9875 and 0.9825) between the PAI estimates proved the reliability of above canopy reference image restoration from below canopy hemispherical image in HSP software for canopy gap fraction estimation.

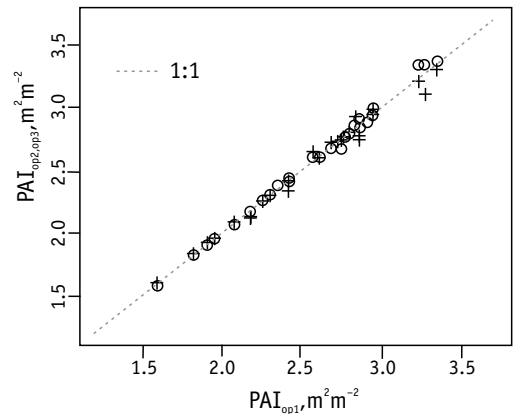


Figure 4. Intercomparison of plant area index estimates of three operators (op1, op2, op3).

Joonis 4. Kolme sõltumatu pilditöötleja (op1, op2, op3) tulemustel saadud taimkatteindeksi PAI võrdlus.

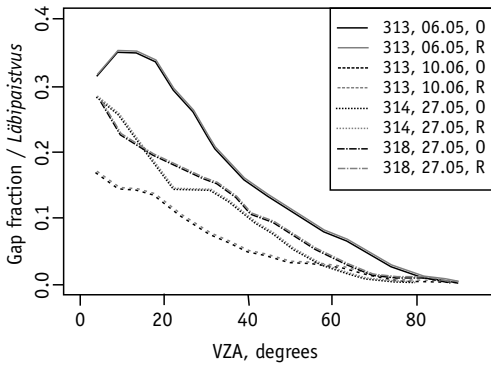


Figure 5. The above canopy sky image is restored by using samples taken from the canopy gaps found in the below canopy image above. The samples from small gaps may contain mixed pixels which introduce negative bias in restored sky radiance image. The differences in gap fraction estimate by using the original point set (O) and after removing few possible erroneous gap markers (R) are small and almost no detectable.

Joonis 5. Väikestes võrastikus olevates aukudes on tihti raske otsustada, kas heleduse variatsioon pildil on põhjustatud taimeosade sattumisest vaatevälja või hoopis pilvedest põhjustatud taeva heleduse muutlikkusest. Algse märgenduse järgi (O) ja mõnede kahtlaste punktide eemaldamise järel korratud (R) läbipaistvuse arvutuse tulemused oluliselt ei erine.

The above canopy sky radiance images created by the restoration method of Lang *et al.* (2010) are, of course, not free from estimation errors. Lang *et al.* (2010) analyzed variability of calculated gap fraction at canopy gap level and found the mean value close to $P_0 = 1.0$ and random errors usually less than 0.05. At pixel level the errors could be larger due to natural variability of sky radiance and differences in sensitivity of camera sensor pixels. Here we analyzed the influence of sky radiance sampling points placed into the gaps with mixed pixels to the sample plot gap fraction estimates and found only marginal changes of gap fraction (Figure 5). Revision of sky

sample points on images from four sample plots showed only a very small influence on plot level gap fraction after removing all of such points which could be influenced by mixed pixels. Few of the sky samples were found from sky/canopy mixed pixels but in many cases it was difficult to decide whether the gap was canopy/sky mixture or whether the variability was due to the clouds. However, the results indicated that the first decision of operators when identifying the small gaps suitable for sky radiance sampling was consistent. The correct measurements of gap fraction at large view zenith angles from hemispherical images, however, remains a challenge due to weak signal, signal distortion in optics and cameras, low spatial resolution compared to near zenith direction and due to variability in sky radiance.

As an example we used gap fraction data from the above canopy sky reference restoration procedure to validate the Nobis-Hunziker automatic thresholding algorithm. Processing of the JPEG files required about 30 seconds per image but the time consumption per linear image data in PGM files ranged between 90 to 240 seconds due to much bigger number of different gray levels compared to the JPEGs. The results revealed a significant dependence of estimated PAI on the input data format and characteristics. Determination coefficient R^2 of linear relationship between JPEG based PAI estimate and LinearRatio based PAI was 0.62 while for the thresholded HSP working files we got $R^2 = 0.83$. The PAI from out of camera JPEG files was underestimated (Figure 6) whereas the PAI derived from the same images which were used in HSP was overestimated. This is somewhat contradictory to the results of Manninen *et al.* (2009) who had to apply -7DN (pixel maximum value in the images was 255DN) correction to the threshold found by Nobis-Hunziker for JPEG images in order to remove the PAI overestimation compared to the LAI-2000 based estimates. In our test we would have to apply exactly

the opposite correction to the threshold for JPEG images to remove bias compared to LinearRatio based PAI. Here we conclude that the behavior of Nobis-Hunziker automatic thresholding algorithm requires further studies.

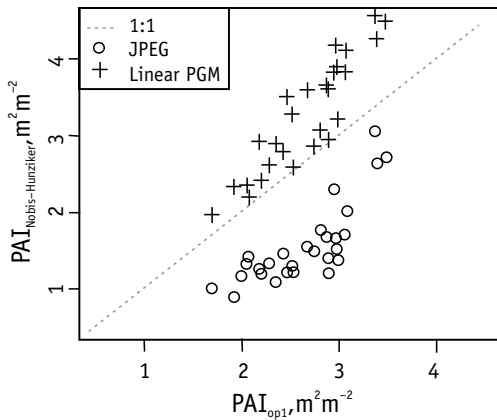


Figure 6. Nobis-Hunziker automatic thresholding algorithm was used to estimate canopy gap fraction from out of camera JPEG files and from the linear radiance data (Linear PGM) extracted from the raw data files. The same images were processed in HSP to calculate PAI_{op1} which was used to validate the automatic thresholding procedure. The validation indicates strong dependence of the automatic thresholding on the input data characteristics.

Joonis 6. Nobis-Hunziker automaatset klassifitseerimisalgoritmi rakendati kaamerates koostatud JPEG piltidele ning toorandmetest eraldatud lineaarsest heleduse ja sensori lugemi seost sisaldavale andmestikule (Linear PGM). Tulemuste kontroll HSP-s arvatud taimkatte läbipaistvuse alusel saadud indeksi PAI_{op1} järgi näitas automaatalgoritmi olulist sõltuvust klassifitseeritava pildi heleduse jaotusest.

Gap fraction measurements are the first step in leaf area index studies. Hence, the errors made in this step propagate into the leaf area index estimates and introduce significant uncertainties independent on the algorithm used for canopy gap fraction data inversion. We tested a new method

(Lang *et al.* 2010) for restoration of above canopy hemispherical image for Cescatti's (2007) LinearRatio and found the method performing well on artificial target and on real below canopy hemispherical images. The method is almost independent on operator's decision, is based on linear measurement data and does not require additional sensor for reference during field measurements. Instead, the second camera can be used for below canopy measurements making the fieldwork and usage of diffuse illumination time more efficient. The image processing in HSP requires a bit more work than just setting a threshold. Our experiences showed that in average five to ten minutes are required to process a single image, however, in future HSP versions the image processing can be fully automated. A small drawback of the above canopy sky restoration data processing in HSP is also the significant consumption of data storage space per sample plot, since about 250MB is required to store e.g. twelve raw data files and the derived gap fraction images. However, modern hard disks can store several terabytes of data which makes the problem less significant. There is also theoretical possibility for gap fraction overestimation in the above canopy sky reference image restoration process if the operator places sky sampling marks to the mixed sky/canopy pixels. This problem, however, can be overcome with preliminary training of image interpretation skills of the operator.

The application software HSP can interface most of popular existing canopy structure indices calculation programs, since HSP can export the gap fraction data and images in different formats. This allows using already tested software for calculating canopy structural indices without modification of the code and abandon the subjective thresholding step found in those programs.

Few comments must be made on using commercial cameras as measurement devices. The plant canopy analyzer LAI-

2000 sensitivity range is suitable for measurements in almost any light conditions, whereas for digital cameras ISO sensitivity, shutter speed and aperture value have to be by set user to keep the recorded signal below sensor saturation. Leblanc (2008) recommends to follow image brightness histogram displayed by the camera. However, we found occasionally signs of signal saturation at 3700 DN in 12-bit Canon EOS 5D images, although the histogram in the camera reached only about 80% of the maximum for the images (see Lclevy, 2013). There is no guarantee that *raw data* is not processed in the camera and is fully comparable to plant canopy analyzer data. Hence, careful testing of cameras and hemispherical optics in radiometry lab before field measurements is recommended.

Acknowledgments. The authors thank Professor Youngryel Ryu and his student Soohyun Jeon from Department of Landscape Architecture and Rural Systems Engineering, Seoul National University, for sharing the image of the perforated panel. Support for the HSP Project Manager software development was provided by Environmental Conservation and Environmental Technology R&D programme project „Aeglaselt kulgevate nähtuste tuvastamise kaugseiremeetodite täiustamine“ (3.2.0801.11-0012) and Estonian Science Foundation grant no ETF8290. Programmers from Callista Software OÜ, Estonia, wrote the HSP software code. The image analysis was supported by Environmental Conservation and Environmental Technology R&D programme project ERMAS and by Institutional Research Funding grant IUT21-04 (B21004MIMK). The authors thank reviewers for their useful comments on the manuscript.

References

- Anderson, M.C. 1964. Studies of the woodland light climate. I. The photographic computation of light condition. – *Journal of Ecology*, 52, 27–41.
- Atkins, W.R.G, Poole, H.H, Stanbury, F.A. 1937. The measurement of the intensity and the colour of the light in woods by means fo emission and rectifier photoelectric cells. – *Proceedings of the Royal Society of London*, 121, 427–450.
- Beerling, D. 2012. The Emerald Planet. How plants changed Earth's history. (Smaragdplaneet. Kuidas tamed on muutnud Maa ajalugu). Tallinn, Kirjastus Varrak. 352 pp. (Translation into Estonian).
- Cescatti, A. 2007. Indirect estimates of canopy gap fraction based on the linear conversion of hemispherical photographs – Methodology and comparison with standard thresholding techniques. – *Agricultural and Forest Meteorology*, 143(1-2), 1–12.
- CIE, 2004. ISO 15469:2004/CIE S 011:2003. Joint ISO/CIE standard: spatial distribution of daylight – CIE standard general sky.
- Coffin, D. 2013. Decoding raw digital photos in Linux. [WWW document]. – URL <http://www.cybercom.net/~dcoffin/dcraw/> [Accessed 10 April 2014].
- Evans, G.C., Coombe, D.E. 1959. Hemispherical and woodland canopy photography and the light climate. – *Journal of Ecology*, 47, 123–144.
- Frazer, G.W., Canham, C.D., Lertzman, K.P. 1999. Gap Light Analyzer (GLA), Version 2.0: Imaging software to extract canopy structure and gap light transmission indices from true-colour fish-eye photographs, user's manual and program documentation. Simon Fraser University, Burnaby, British Columbia; The Institute of Ecosystem Studies, Millbrook, New York.
- Hordo, M., Kiviste, A., Sims, A. 2006. The network of permanent sample plots for forest growth in Estonia. – Nagel, J. (ed.). *Deutscher Verband Forstlicher Forschungsanstalten: DVFFA – Sektion Ertragskunde, Staufen, May 29–31, 2006, Germany*, 115–121.
- Jonckheere, I., Fleck, S., Nackaerts, K., Muys, B., Coppin, P., Weiss, M., Baret, F. 2004. Review of methods for in situ leaf area index determination Part I. Theories, sensors and hemispherical photography. – *Agricultural and Forest Meteorology*, 121, 19–35.
- Jonckheere, I., Nackaerts, K., Muys, B., Coppin, P. 2005. Assessment of automatic gap fraction estimation of forests from digital hemispherical photography. – *Agricultural and Forest Meteorology*, 132, 96–114.
- Inoue, A., Yamamoto, K., Mizoue, N., Kawahara, Y. 2004. Effects of image quality, size and camera type on forest light environment estimates using digital hemispherical photography. – *Agricultural and Forest Meteorology*, 126(1–2), 89–97.

- Kittler, R. 1994. Some qualities of scattering functions defining sky radiance distributions. – *Solar Energy*, 53(6), 511–516.
- Kuusik, A., Nilson, T., Paas, M. 2002. Angular distribution of radiation beneath forest canopies using a CCD-radiometer. – *Agricultural and Forest Meteorology*, 110(4), 259–273.
- Lang, M., Kuusik, A., Möttus, M., Rautiainen, M., Nilson, T. 2010. Canopy gap fraction estimation from digital hemispherical images using sky radiance models and a linear conversion method. – *Agricultural and Forest Meteorology*, 150(1), 20–29.
- Lclevy. 2013. Understanding what is stored in a Canon RAW .CR2 file, How and why (.CR2 files are produced by Canon EOS digital cameras since 2004). Version 0.72 (August 30th, 2013). [WWW document]. – URL <http://lclevy.free.fr/cr2/index.html#wb> [Accessed 10 April 2014].
- Lebourgeois, V., Bégué, A., Labbé, S., Mallavan, B., Prévot, L., Roux, B. 2008. Can Commercial Digital Cameras Be Used as Multispectral Sensors? A Crop Monitoring Test. – *Sensors*, 8, 7300–7322.
- Leblanc, S.G., Chen, J.M., Fernandes, R., Deering, D.W., Conley, A. 2005. Methodology comparison for canopy structure parameters extraction from digital hemispherical photography in boreal forests. – *Agricultural and Forest Meteorology*, 129(3–4) 187–207.
- Leblanc, S.G. 2008. DHP-TRACWin Manual. Natural Resources Canada, Canada Centre for Remote Sensing, 29 pp.
- Lõhmus, E. 2004. Eesti metsakasvukohatüübid. (Forest site types in Estonia). Tartu, Eesti Loodusfoto. 80 pp. (In Estonian).
- Macfarlane, C., Michael Coote, M., White, D.A., Adams, M.A. 2000. Photographic exposure affects indirect estimation of leaf area in plantations of *Eucalyptus globulus* Labill. – *Agricultural and Forest Meteorology*, 100(2–3), 155–168.
- Macfarlane, C., Hoffman, M., Eamus, D., Kerp, N., Higginson, S., McMurtrie, R., Adams, M. 2007a. Estimation of leaf area index in eucalypt forest using digital photography. – *Agricultural and Forest Meteorology*, 143(3–4), 176–188.
- Macfarlane, C., Grigg, A., Evangelista, C. 2007b. Estimating forest leaf area using cover and fullframe fisheye photography: Thinking inside the circle. – *Agricultural and Forest Meteorology*, 146 (1–2), 1–12.
- Manninen, T., Korhonen, L., Voipio, P., Lahtinen, P., Stenberg, P. 2009. Leaf area index (LAI) estimation of boreal forest using wide optics airborne winter photos. – *Remote Sensing*, 1, 1380–1394.
- Niinemets, Ü., Ellsworth, D.S., Lukjanova, A., Tobias, M. 2001. Site fertility and the morphological and photosynthetic acclimation of *Pinus sylvestris* needles to light. – *Tree Physiology*, 21, 1231–1244.
- Nilson, T. 1971. A theoretical analysis of the frequency of gaps in plant stands. – *Agricultural and Forest Meteorology*, 8, 25–28.
- Nilson, T., Kuusik, A. 2004. Improved algorithm for estimating canopy indices from gap fraction data in forest canopies. – *Agricultural and Forest Meteorology*, 124(3–4), 157–169.
- Nobis, M., Hunziker, U. 2005. Automatic thresholding for hemispherical canopy-photographs based on edge detection. – *Agricultural and Forest Meteorology*, 128, 243–250.
- Pisek, J., Lang, M., Nilson, T., Korhonen, L., Karu, H. 2011. Comparison of methods for measuring gap size distribution and canopy nonrandomness at Järvselja RAMI (RADiation transfer Model Inter-comparison) test sites. – *Agricultural and Forest Meteorology*, 151(3), 365–377.
- Rich, P.M. 1990. Characterizing plant canopies with hemispherical photographs. – *Remote Sensing Reviews*, 5, 13–29.
- Ryu, Y., Sonnentag, O., Nilson, T., Vargas, R., Kobayashi, H., Wenk, R., Baldocchi, D.D. 2010. How to quantify tree leaf area index in an open savanna ecosystem: A multi-instrument and multi-model approach. – *Agricultural and Forest Meteorology*, 150(1), 63–76.
- Song, G.-Z. M., Doley, D., Yates, D., Chao, K.-J., Hsieh, C.-F. 2014. Improving accuracy of canopy hemispherical photography by a constant threshold value derived from an unobserved overcast sky. – *Canadian Journal of Forest Research*, 44, 17–27.
- Schleppi, P., Conedera, M., Sedivy, I., Thimonier, A. 2007. Correcting non-linearity and slope effects in the estimation of the leaf area index of forests from hemispherical photographs. – *Agricultural and Forest Meteorology*, 144, 236–242.
- Tooming, H. 1977. Солнечная радиация и формирование урожая. (Solar radiation and crop yield production). Leningrad, Gidrometeoizdat. 200 pp. (In Russian).
- Walter, J.-M. 2009. CIMES-FISHEYE – hemispherical photography of forest canopies. [WWW document]. – URL <http://jmnw.free.fr> [Accessed 10 April 2014]. Université de Strasbourg, Faculté des Sciences de la Vie, Institut de Botanique, 28 Rue Goethe, 67083 Strasbourg Cedex France.
- Watson, D.J. 1947. Comparative physiological studies in the growth of field crops. I. Variation in net assimilation rate and leaf area between species and varieties, and within and between years. – *Annals of Botany*, 11, 41–76.
- Weiss, M. 2013. Welcome to the CAN-EYE web site. [WWW document]. – URL <https://www4.paca.inra.fr/can-eye> [Accessed 10 April 2014].
- Welles, J.M., Norman, J.M. 1991. Instrument for indirect measurement of canopy architecture. – *Agronomy Journal*, 83, 818–825.
- Wilson, J.W. 1960. Inclined point quadrats. – *New Phytologist*, 59, 1–7.

Metsa võrastiku läbipaistvuse mõõtmine digitaalsete poolsfäärikaamerate abil

Mait Lang, Ave Kodar ja Tauri Arumäe

Kokkuvõte

Fotosünteesiprotsessi käigus neelduva kiirguse hulk ja tekkinud biomass on hästi seotud roheliste lehtede pindalaga taimkattes (Tooming, 1977). Atkins *et al.* (1937) kasutasid fotoelemente metsas võrastikust läbi tulnud kiirguse mõõtmiseks, et iseloomustada võrastiku läbipaistvust $T = I_b/I_0$ kus I_0 ja I_b on vastavalt lagedal ja metsa all mõõdetud kiirguse tugevused. Evans & Coombe (1959) testisid vertikaalsuunas orienteeritud erilist poolsfääri optikaga filmikaamerat võrastiku seisundi jäädvustamiseks. Anderson (1964) näitas, et kui poolsfäärifoto jagada sektoriteks vaatesuuna asimuudi ning seniitnurga järgi ja igale sektorile anda visuaalselt läbipaistvuse hinnang, siis üle kõikide sektorite keskmistatud väärtus kirjeldab väga hästi võrastiku läbipaistvust. Lehtede hulga kirjeldamiseks kasutatakse lehepinnaindeksit (LAI), mis arvutatakse lehtede ühepoolse pindala ja taimkatte aluse pindala suhtena (Watson, 1947), mida varasemalt on mõõdetud kaldnõel meetodiga (Wilson, 1960), kus registreeritakse lehtede ja pika peenikese nõela kontakte. Nilson (1971) näitas, et võrastikus olevate aukude keskmise osakaalu P_0 (ka tõenäosus, et kontakte ei ole) ja LAI seost kirjeldab teoreetiline võrrand (1), kus k on kiirguse nõrgenemistegur. Poolsfääripiltidelt (varasemalt digitaliseeritud fotod) on hinnatud P_0 väärtust klassifitseerides pikslid heleduse järgi klassideks taevas $P_0 = 1$ ja leht ehk taim $P_0 = 0$. Niinimetatud optimaalse läve ehk eristusnivoo (*threshold*) leidmine aga on jäänudki lahendamatuks probleemiks (Anderson, 1964; Rich, 1990; Jonckheere *et al.*, 2004, 2005), kuigi mõnedel juhtudel on isegi automaatsete algoritmidega saadud päris häid tulemusi (Manninen *et al.*, 2009).

Põhimõttelise lahenduse kahe digitaalse kaameraga võrastiku läbipaistvuse mõõtmiseks töötas välja Cescatti (2007), kes näitas et modernsete digikaamerate salvestatavas toorandmestikus (*raw data*) on signaali tugevus lineaarselt seotud pealelangeva kiirguse hulga ja rakendada saab sarnaselt Atkins *et al.* (1937) kasutatuga lagedal ja metsas mõõtvat sensori tehnikat. Sarnane mõõtmis skeem on kasutusel ka taimkatteanalüsaatorites (Welles & Norman, 1991).

Käesolevas töös testiti programmis HemisSpherical Project Manager (HSP) realiseeritud lahendust, kus Cescatti (2007) meetod on kohandatud ühe, vaid metsa all mõõtvat kaamera jaoks (Lang *et al.*, 2010). Taimkatte pealne kujutis ennustatakse interpoolimise ja sama pildi jaoks lähendatud taeva heleduse mudeli (CIE, 2004) abil võrastiku aukudes olevate katmata taeva heleduse väärtuste järgi (Lang *et al.*, 2010). Testiti perforeeritud, teadaoleva aukude osakaaluga (0,4030) pilves taeva taustal pildistatud paneeli (joonis 1) aukude osakaalu hindamist. Igast augu keskelt võeti taeva heleduse näidis. Kõigi 179 näidise järgi saadud katmata taeva kujutise korral oli paneeli $P_0 = 0,3792$, kümnes katses 17 juhuslikult valitud punkti ja teave heleduse mudeli kasutamisel oli keskmiselt paneeli $P_0 = 0,3826$ ja standardhälve $S_{p_0} = 0,0114$. Nobis & Hunziker (2005) automaatse klassifitseerimisalgoritmi järgi leitud taeva ja paneeli eristusnivoo 1315 DN heleduse järgi andis paneeli $P_0 = 0,3696$. Tootja spetsifikatsioonist väiksema aukude osakaalu põhjuseks on arvatavasti aukude külgedel olevad defektid ja teisalt võibki paneeli tegelik P_0 olla veidi väiksem arvestades spetsifikatsioonis lubatud veapiire. Metsa

kasvukäigu proovitükkidel Laevas (tabel 1) tehti 2013. aasta varakevadest suveni (joonised 2, 3) poolsfääripilte ning saadud andmestikku töötlesid kolm sõltumatut operaatorit. Ainsaks reegliks oli, et matemaatilise mudeli osakaal pidi olema alla 0,3. Iga mõõtmiskorra kohta arvutati valemiga (2) igal proovitükil taimkatteindeks (PAI). Operaatorite võrdlus näitas, et HSP-s realiseeritud meetodika on objektiivne ning ei sõltu eriti oluliselt andmeid töötlevast operaatorist (joonis 4), mis oli põhimõtteliseks probleemiks lävemeetodi korral. Väikestest võrastiku aukudest võetud taeva näidised võivad sisaldada okste ja taeva segupiksleid. Segupikslike sattumisel katmata taeva näidiste hulka hinnatakse läbipaistvust tegelikust suuremaks. Nelja proovitüki puhul tehti korduskatse, kus eemaldati kõik vähegi kahtlust tekitanud näidised (neid ei olnud palju) ja tuletati uus taimkatte pealne pilt. Võrdluses algse läbipaistvuse hinnanguga olulist vahet ei olnud (joonis 5). Pildilt on samas raske otsustada, kas väikesed augud võrastikus on lage taevas, mille heleduse variatsioo-

ni põhjustavad pilved, või lehtede ja taeva segu. Suurte seniitnurkade jaoks metsa läbipaistvuse täpsem mõõtmine jääb seega ka edaspidiseks keeruliseks ülesandeks. HSP-s arvatatud taimkatte läbipaistvuse andmeid kasutati Nobis-Hunziker automaatse klassifitseerimisalgoritmi valideerimiseks ja tuvastati algoritmi oluline sõltuvus pildi pikslike heleduse jaotusest (joonis 6). Kokkuvõttes järeldati, et HSP-s oleva metsa võrastiku läbipaistvuse arvutamise meetodika on objektiivne ja seda tuleks edaspidi kasutada paljude taimkatte struktuuriindeksite arvutamise programmide (GLA (Frazer *et al.*, 1999), CIMES (Walter, 2007), CanEye (Weiss, 2013), hemispher (Schleppi *et al.*, 2007) ja DHP (Leblanc *et al.*, 2005) sisendis oleva subjektiivse klassifitseerimistehnika asemel. Edaspidistes uurimustes tasuks tähele panna, et digikaamerates võib toimuda ka toorandmestiku eeltöötlus viisil, mis ei taga toorandmestiku lineaarseost optikasüsteemi sisenenud kiirgusega. Seetõttu on soovitatav taimkatte läbipaistvuseks mõeldud kaameraid eelnevalt radiomeetrialaboris testida.

Received April 14, 2014, revised May 5, 2014, accepted May 28, 2014